

See discussions, stats, and author profiles for this publication at: <https://www.researchgate.net/publication/271918814>

VBEFP/PCM: A QM/MM/PCM approach for valence-bond method and its application for the vertical excitations of formaldehyde and acetone in aqueous solution

ARTICLE *in* SCIENCE CHINA-CHEMISTRY · OCTOBER 2014

Impact Factor: 1.7 · DOI: 10.1007/s11426-014-5192-x

READS

19

4 AUTHORS, INCLUDING:



Peifeng Su

Xiamen University

22 PUBLICATIONS 602 CITATIONS

SEE PROFILE



Wei Wu

Xiamen University

102 PUBLICATIONS 2,032 CITATIONS

SEE PROFILE

VBEFP/PCM: a QM/MM/PCM approach for valence-bond method and its application for the vertical excitations of formaldehyde and acetone in aqueous solution

HUANG Jing, YING FuMing, SU PeiFeng* & WU Wei*

The State Key Laboratory of Physical Chemistry of Solid Surfaces, Fujian Provincial Key Laboratory of Theoretical and Computational Chemistry and College of Chemistry and Chemical Engineering, Xiamen University, Xiamen 361005, China

Received March 20, 2014; accepted June 28, 2014

In this paper, a combined QM/MM/PCM approach, named VBEFP/PCM, is presented for *ab initio* VB study with a solvent effect incorporated. In VBEFP/PCM, both short-range and long-range solvent effects are taken into account by effective fragment potential (EFP) and polarizable continuum model (PCM), respectively, while the solute molecules are described by valence bond (VB) wave function. Furthermore, VBEFP/PCM, along with VBPCM and VBEFP, is employed for the $n \rightarrow \pi^*$ vertical excitation of formaldehyde and acetone molecules in aqueous solution. The computational results show that VBEFP/PCM can provide the appropriate solvent shifts, whereas VBPCM underestimates the solvent shifts due to its lack of short-range solvent effect. The VBEFP results strongly rely upon the description of the short-range solvent effect. To explore the role of the solute's electronic structure in the solvent shift, resonance energy analysis during the excitation is performed. It was found that the solute's electronic polarization plays the most important role in the solvent shift. The π resonance controls the variation of the solute's wave function during the $n \rightarrow \pi^*$ vertical excitation, which leads to the blue solvent shifts.

***ab initio* valence bond, solvent effects, VBEFP/PCM, solvent shifts**

1 Introduction

Solvent effect has been a subject of theoretical chemistry due to its vital role in most chemical and biochemical processes [1]. In general, solvent effects can be divided into two categories. The first one is the long-range solvent effect, which can be considered as electrostatic interaction among solute-solvent molecules. It can be simulated theoretically by continuum solvation models, in which solvent molecules are represented as a homogeneous medium and polarized by the charge distribution of the solute [2]. For valence bond (VB) methods, VBPCM [3] and VBSM [4] are based on the continuum solvation models PCM [5] and SMx [6, 7], respectively. Therefore, the long-range solvent effect is

included in VB scheme.

The second category is the short-range solvent effect, denoted as special interactions among solute molecules and the surrounding solvent molecules. It can be treated theoretically by discrete models in which solvent molecules are explicitly considered. Discrete methods can be combined with quantum mechanical methods to achieve QM/MM calculations for investigating special solute-solvent interactions [8] such as hydrogen bonding or solvent coordination, with a balance of computational accuracy and efficiency. Recently, a QM/MM type VB method, named VBEFP, was presented for *ab initio* VB calculations with explicit solvent effects [9]. In VBEFP, the EFP1 method, a polarized force-field approach developed by Gordon *et al.* [10] is employed for the MM part (environment), while the VBSCF method is used for the QM part of the system.

Because they utilize the advantages of the continuum

*Corresponding authors (email: supi@xmu.edu.cn; weiwu@xmu.edu.cn)

solvation models and the discrete models, combined continuum-discrete solvation approaches can provide a practical way to properly describe the whole solvated environment properly [11]. As one kind of discrete/continuum solvation method, the QM/EFP/PCM scheme was developed by Gordon *et al.* [12] and Li *et al.* [13]; here, the long-range solvent effect can be treated by PCM while the short-range solvent effect is handled by EFP.

In this paper, the QM/MM/PCM scheme is applied to the *ab initio* VB method, named VBEFP/PCM, in which the VB method is adopted as the QM method. This scheme enables the investigation of the chemical processes in complicated solvated environments by the VB approach.

In general, vertical excitation in polar solution leads to solvent shifts. The origin of the blue solvent shift for the $n \rightarrow \pi^*$ vertical excitation of formaldehyde and acetone in polar solvent has been investigated extensively by various theoretical approaches, involving MD\MC simulations [14, 15], discrete/continuum solvation approaches [16–18], and non-equilibrium implicit solvation approaches [19, 20]. As for the origin of the blue solvent shift, most theoretical studies have focused on the discussion of the solute-solvent interaction. Less attention has been paid to the role of the solute’s electronic structures, although this has been noticed by a few researchers [21, 22]. Using Car-Parrinello molecular dynamics (CPMD) and QM/MM computations, Carloni *et al.* [21] emphasized that the blue shift of formaldehyde in aqueous solution is totally attributed to the polarization of the wave functions. Xu *et al.* [22] claimed that the solute polarizability contributes about 35% of the total solvent shift for formaldehyde. These inconsistencies, which show that the role of solute’s electronic structures in solvent shift are still not clearly understood, serves as another motivation for this paper.

In this paper, the VBEFP/PCM method is employed for the $n \rightarrow \pi^*$ vertical excitation of formaldehyde and acetone in aqueous solution, along with VBEFP and VBPCM calculations. Following theoretical studies [16–18, 23, 24], up to two water molecules are used for the hydrogen bonds among the O atom and the surrounding water molecules in the VBEFP and VBEFP/PCM calculations. The role of the electronic structures of the solute molecule for the solvent shift is explored by analyzing the wave function of the solute molecule, particularly through resonance energy analysis.

2 Theory and methodology

2.1 VB methodology

In VB theory, a many-electron wave function is expressed in terms of VB functions [25].

$$\Psi^{\text{VB}} = \sum_K C_K \Phi_K \quad (1)$$

where VB function Φ_K corresponds to a classic VB structure that can be expressed as follows:

$$\Phi_K = \hat{A} \Omega_0 \Theta_K \quad (2)$$

where \hat{A} is an antisymmetrizer, Ω_0 is a direct product of orbitals $\{\varphi_i\}$ as:

$$\Omega_0 = \varphi_1(1)\varphi_2(2)\cdots\varphi_N(N) \quad (3)$$

and Θ_K is a spin-paired spin eigenfunction, defined as:

$$\Theta_K = 2^{-1/2} [\alpha(k_1)\beta(k_2) - \beta(k_1)\alpha(k_2)] \times 2^{-1/2} [\alpha(k_3)\beta(k_4) - \beta(k_3)\alpha(k_4)] \cdots \alpha(k_p) \cdots \alpha(k_N) \quad (4)$$

In Eq. (4), the scheme of spin pairing (k_1, k_2) , (k_3, k_4) , etc., corresponds to the bond pairs describing the structure K .

C_K in Eq. (1) can be obtained by the following secular equation:

$$\mathbf{H}\mathbf{C} = \mathbf{E}\mathbf{M}\mathbf{C} \quad (5)$$

where \mathbf{H} , \mathbf{M} , and \mathbf{C} are the Hamiltonian, overlap, and coefficient matrix, respectively. Hamiltonian and overlap matrix elements are defined as:

$$\mathbf{H}_{KL} = \langle \Phi_K | \hat{H} | \Phi_L \rangle \quad (6)$$

and

$$\mathbf{M}_{KL} = \langle \Phi_K | \Phi_L \rangle \quad (7)$$

In the VBSCF method, both the structure coefficients and VB function shown in Eq. (1) are simultaneously optimized to minimize the total energy. The VB functions are optimized via the occupied orbitals, which are usually expanded as linear combination of basis functions:

$$\varphi_i = \sum_{\mu} T_{\mu i} \chi_{\mu} \quad (8)$$

2.2 The VBEFP/PCM scheme

In the VBEFP/PCM scheme, the molecular cavity is constructed by solute-solvent complex, which means that it is represented by the solute itself plus the solvent molecules introduced by the EFP model. As proposed by Li *et al.* [13], the EFP-induced dipoles and the PCM-induced charges are solved iteratively. The potential describing the interaction between the QM-EFP part and the PCM part can be expressed as:

$$V^{\text{EFP/PCM}} = V^{\text{ele}} + V^{\text{N}} + V^{\text{Mul}} + V^{\text{Pol}} \quad (9)$$

where $V^{\text{EFP/PCM}}$ contains four terms: the electronic term V^{ele} , the nuclear term V^{N} , the Coulomb interaction term by multipole expansion V^{Mul} , and the EFP induced-dipole term V^{Pol} . V^{ele} and V^{N} come from the QM part, and V^{Mul} and V^{Pol} come

from the EFP part.

With VBEFP/PCM, the total free energy is expressed as:

$$E^{\text{VBEFP/PCM}} = \langle \Psi^{\text{VBEFP/PCM}} | \hat{H} + V^{\text{EFP}} | \Psi^{\text{VBEFP/PCM}} \rangle + \Delta G^{\text{ele}} \quad (10)$$

where V^{EFP} represents the interaction between the QM and EFP parts [13]. Thus ΔG^{ele} can be written as:

$$\Delta G^{\text{ele}} = \frac{1}{2} (V^{\text{ele}} + V^{\text{N}} + V^{\text{Mul}} + V^{\text{Pol}}) \cdot (q^{\text{ele}} + q^{\text{N}} + q^{\text{Mul}} + q^{\text{Pol}}) \quad (11)$$

q^{ele} , q^{N} , q^{Mul} , and q^{Pol} are the induced charge by the potentials V^{ele} , V^{N} , V^{Mul} , and V^{Pol} , respectively.

The computational procedure of VBEFP/PCM is shown in Figure 1.

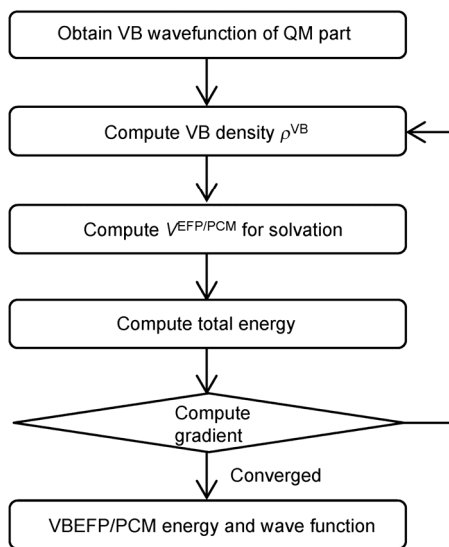


Figure 1 Flow chart of the VBEFP/PCM scheme.

3 Computational details

The optimization calculations are performed with the GAMESS-US program package [26]. The B3LYP/6-31G*-optimized geometries of the $\text{CR}_2\text{O} \cdot n\text{H}_2\text{O}$ complexes ($\text{R} = \text{H}$ or CH_3 , $n = 0-2$) with the key geometrical parameters, in which there are extinct hydrogen bonds between the O atom and the solvent water molecule, are shown in Figure 2. In the VBPCM and VBEFP/PCM calculations, the conductor-like polarizable continuum model (CPCM) method is employed [27]. The solute's cavity is constructed by the fixed points with variable areas (FIXPVA) tesserae scheme [28]. The dielectric constant ϵ is set as 78.4 for the water environment. The universal force field (UFF) radii model scaled by a factor of 1.1 is employed [29]. Using the recently developed orbital optimization algorithms [30–32], the VB calculations are performed by XMVB module [33, 34] at the VBSCF/6-31G* level by the GAMESS-US program package [26].

All the valence electrons (12 for formaldehyde and 24 for acetone) are involved in the VB calculations. The VB orbitals are strictly localized on the O atom and the CR_2 ($\text{R} = \text{H}$ or CH_3) groups. The C=O bonding is shown in Figure 3, in which the C and O atoms lie on the z-axis. The two H atoms of formaldehyde and two CH_3 groups of acetone, which are not explicitly shown in Figure 3, are located at the y-z plane. The p_x atomic orbitals (AOs) of both O and C atoms are in the plane of the paper, whereas the p_y AOs are drawn as circles pointing at the observer. Eight and 14 VB orbitals are employed for formaldehyde and acetone, respectively. Among these VB orbitals, six are treated as active orbitals for the ground and first excited states, which involve two p_σ -type, two p_x , and two p_y orbitals.

For a system of spin S with N electrons and m orbitals,

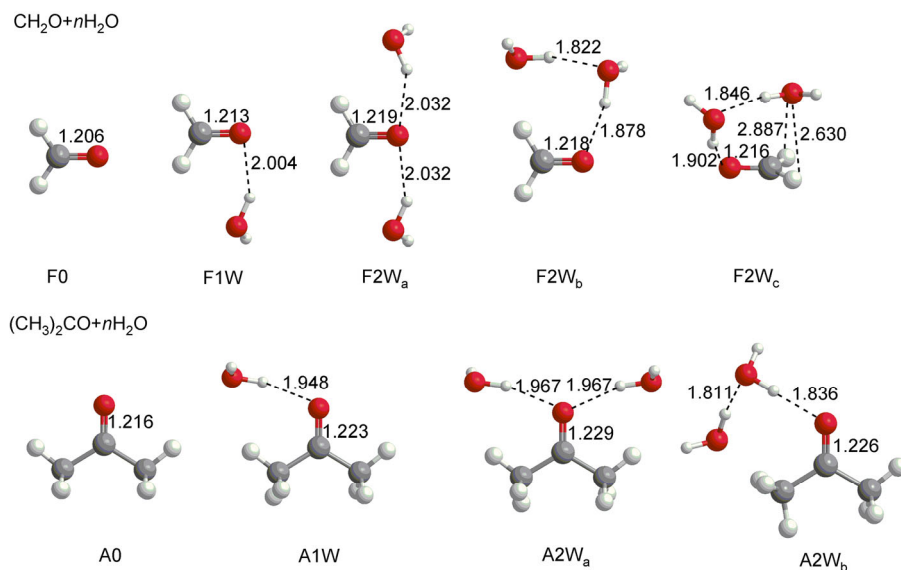


Figure 2 Optimized parameters of $\text{CR}_2\text{O} \cdot n\text{H}_2\text{O}$, ($\text{R} = \text{H}$ or CH_3 , $n = 1, 2$) at the B3LYP/6-31G* level (Å).

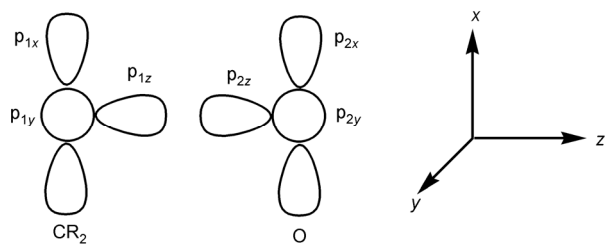


Figure 3 VB orbital description of CR_2O ($\text{R} = \text{H}$ or CH_3).

the number of independent VB structures is given by the Weyl formula [35]:

$$D(m, N, S) = \frac{2S+1}{m+1} \binom{m+1}{\frac{1}{2}N+S+1} \binom{m+1}{\frac{1}{2}N-S} \quad (12)$$

For the singlet-ground-state of the CR_2O ($\text{R} = \text{H}$ or CH_3) molecules, if we take all six active orbitals and eight active electrons into account for the $\text{C}=\text{O}$ bonding, we obtain a total of 105 VB structures. As applied in the previous VB studies [36–38], two strategies, one quantitative and the other qualitative, can be employed to select the most important VB structures for the system at hand. The quantitative strategy is to perform a VBSCF calculation with a complete active set of VB structures, and then to select a restricted set of VB structures according to their weights in the total wave function. The qualitative strategy consists of choosing a restricted set of VB structures, based on chemical grounds, in order to consistently describe the various bonds of the electronic state under study. In this study, these two strategies are employed for both the ground state (S_0) and the $n \rightarrow \pi^*$ excited state (S_1).

For the S_0 state, the p_σ orbitals of the C and O atoms form a σ bond and the $2p_x$ orbitals form a π bond, which leads to the generic structure **1** (Table 1) in which the O atom and CR_2 ($\text{R} = \text{H}$ or CH_3) group keep their neutrality. Because only the equilibrium geometry is required, the alternative coupling of this four-electron, four-orbital system is unimportant and neglected. Structures **2** and **3** in Table 1 are the ionic components of the σ bond, in addition to the covalent component. Similarly, the π bond also has two ionic components, which correspond to the VB structures **4** and **5**. If the ionic resonance forms of the VB structures **2–5** are taken into consideration, six VB structures come into being. Further removal of the high-lying di-ionic structures of the type $\text{C}^{2-}\text{O}^{2+}$ leads to the selection of VB structures **6–8**. Accordingly, the eight 8 structures are chosen in the ground-state calculation. By performing the full VBSCF calculations with 105 VB structures for the ground state, the eight 8 VB structures shown in Table 1 have the largest weights and cover 99% of the total 105 VB structures. Therefore, the two ways lead to the same VB set for the S_0 state.

For the S_1 state, one electron of the lone p_{2y} pair transits to the orbital composed of p_{1x} and p_{2x} . Structure **1'** shown in Table 2 is the generic structure for the S_1 state, where the two unpaired electrons on z -axis form a σ bond, meanwhile the other two electrons are singly coupled and located on the x - z plane and y - z plane, respectively. Structures **2'** and **3'** are the σ ionic forms of Structure **1'**. Based on structures **1'–3'**, the corresponding resonance structures **4'–9'** will be generated after removing structures that are for $\text{C}^{2-}\text{O}^{2+}$ or more unstable electronic configurations. Thus the 9 VB structures shown in Table 2 are selected. By performing the VBSCF calculations with all 105 VB structures at the first excited state, the selected 9 VB structures have the largest weights and cover 99% of the total wave function.

Therefore, the eight and nine VB structures shown in Tables 1 and 2 are selected as the VB wave function for the S_0 and S_1 states, respectively.

4 Results and discussion

4.1 The vertical excitation energies and solvent shifts

The vertical excitation energies (VEE) of formaldehyde and acetone are displayed in Table 3. For the gas phase, the experimental values of the vertical excitation energies are 4.22 [39] or 4.07 eV [40] for formaldehyde and 4.38 [40] or 4.49 eV [41] for acetone. The computed VBSCF values, 4.37 eV for formaldehyde and 4.69 eV for acetone, are close to the experimental data with small deviations.

For the condensed phase, the experimental value is 4.69 eV [42] for acetone and unavailable for formaldehyde [43]. The VEE values of VBPCM are 4.44 and 4.79 eV for formaldehyde and acetone, respectively, and the VBEFP results are greater than their corresponding VBPCM ones. For example, with one explicit water molecule, the VBEFP values of F1W and A1W are 4.47 and 4.83 eV, respectively. Most of the VBEFP values with two explicit water molecules are larger than those with one water molecule. As for VBEFP/PCM, the VEE values are larger than the corresponding VBEFP results. For example, the VEE values of F1W and A1W are 4.52 and 4.90 eV, respectively, which are larger than those of VBEFP.

The solvent shifts are shown in Table 4. For formaldehyde, solvent shifts in aqueous solution are experimentally absent [43] and 1129–1998 cm^{-1} by various computational results [22, 44, 45]. For acetone, the solvent shift experimentally is 1500–1600 cm^{-1} [41, 42, 46, 47] and 1103–2936 cm^{-1} in various theoretical studies [16, 18, 48–50].

The VBPCM solvent shifts of formaldehyde and acetone are 578 and 781 cm^{-1} , respectively, which shows that the VB calculation with only long-range solvent effect is inadequate for solvent shift. With the short-range solvent effect VBEFP provides larger solvent shifts than the VBPCM ones. In detail, the VBEFP solvent shifts for the two explicit

Table 1 The VB structures for the S_0 state of CR_2O ($R = H$ or CH_3)

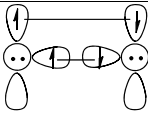
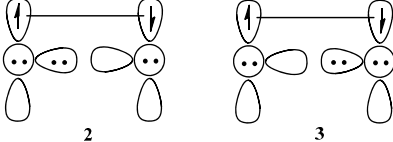
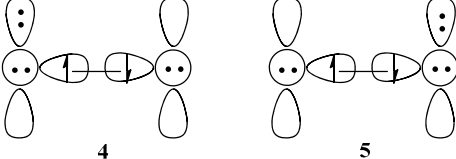
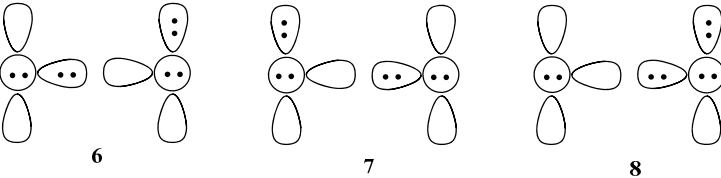
Bonding patterns	VB structures
basic chemical bonding	
σ resonance	
π resonance	
σ - π resonance	

Table 2 The VB structures for the S_1 state of CR_2O ($R = H$ or CH_3)

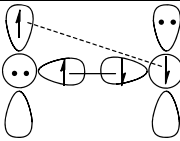
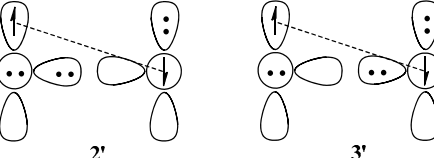
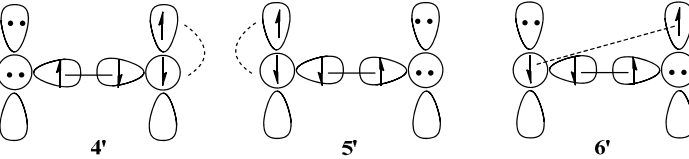
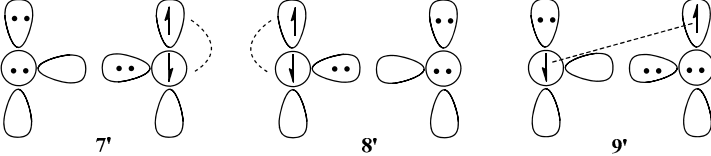
Bonding patterns	VB structures
basic chemical bonding	
σ resonance	
π resonance	
σ - π resonance	

Table 3 The vertical excitation energies (eV) of formaldehyde and acetone

	VBSCF	VBPCM	VBEFP				VBEFP/PCM			
Formaldehyde	GAS	F0	F1W	F2W _a	F2W _b	F2W _c	F1W	F2W _a	F2W _b	F2W _c
	4.37	4.44	4.47	4.56	4.46	4.70	4.52	4.60	4.50	4.73
Acetone	GAS	A0	A1W	A2W _a	A2W _b		A1W	A2W _a	A2W _b	
	4.69	4.79	4.83	4.95	4.85		4.90	5.00	4.91	

Table 4 The solvent shifts (cm^{-1}) of formaldehyde and acetone in aqueous solution

	VBPCM		VBEFP			VBEFP/PCM			
Formaldehyde	F0	F1W	F2W _a	F2W _b	F2W _c	F1W	F2W _a	F2W _b	F2W _c
	578	825	1582	728	2692	1261	1838	1058	2940
Acetone	A0	A1W	A2W _a	A2W _b		A1W	A2W _a	A2W _b	
	781	1096	2085	1279		1715	2492	1752	

water molecules, ranging from 728 to 2692 cm^{-1} for formaldehyde and from 1279 to 2085 cm^{-1} for acetone, greatly depend on the microstructures of the solvent-solute clusters. According to the experimental data and the other computational results mentioned above, the VBEFP values of F1W, F2W_b, A1W, and A2W_b are underestimated. By contrast, VBEFP/PCM provides solvent shifts ranging from 1715 to 2492 cm^{-1} for acetone and from 1058 to 2940 cm^{-1} for formaldehyde, which are larger than the corresponding VBEFP ones. Compared to the VBEFP data, the VBEFP/PCM solvent shifts of F1W, F2W_b, A1W, and A2W_b are more reliable. Furthermore, the solvent shift of A2W_a is 2492 cm^{-1} by VBEFP/PCM is close to the other results on the same geometrical conformation, such as 2500 cm^{-1} by Li [16] with TDB3LYP/EFP/PCM and 2936 cm^{-1} with TD-M06/PCM (SMD) by Truhlar *et al.* [18].

In general, VBEFP/PCM is able to provide the proper solvent shifts but VBPCM cannot. Compared to VBEFP/PCM, the VBEFP results show a relatively large range due to its strong dependence on the short-range solvent-solute interaction. All results satisfy the trend that solvent effect enlarges the solvent-shift values and, in more detailed consideration, larger solvent-shift values. The short-range solvent effect is more important than the long-range one.

4.2 The relationship between the resonance energies and the solvent shifts

As is well known, resonance theory provides a powerful tool for exploring the nature of chemical bonding. Thus, the quantitative specification of the resonance effect is helpful for understanding the solute's electronic polarization from the S_0 to S_1 states. The VB structures shown in Tables 1 and 2 can be further divided into four groups, according to their bonding patterns. The first one contains all of the VB structures, denoted as Group A. Group B includes structures **1** and **1'** for the S_0 and S_1 state, respectively, which shows the fundamental bonding pattern of the ground and excited states, respectively. Group C involves structures **1–3** for the S_0 state and **1'–3'** for the S_1 state. Group D contains **1–5** for the S_0 state and **1'–6'** for the S_1 state.

Thus, various resonance energies including the total, σ , π , and σ - π concerted, can be defined, respectively, as:

$$B_{\text{tot}} = E(\text{B}) - E(\text{A}) \quad (13)$$

$$B_{\sigma} = E(\text{B}) - E(\text{C}) \quad (14)$$

$$B_{\pi} = E(\text{C}) - E(\text{D}) \quad (15)$$

$$B_{\sigma-\pi} = E(\text{D}) - E(\text{A}) \quad (16)$$

where $E(X)$ denotes the energy of the Group X when $X = \text{A}, \text{B}, \text{C}, \text{or D}$.

The computed resonance energies are shown in Table 5. First, the resonance energy in the S_0 state is more sensitive to the solvent effects than in the S_1 state. For the S_0 state, from the gas phase to the aqueous solution, the values of B_{π} and B_{σ} increase, which leads to the increase of B_{tot} . For example, for acetone, the B_{tot} value is 95.4 kcal/mol by VBPCM for A0, 99.7 and 100.5 kcal/mol by VBEFP and VBEFP/PCM, respectively; for A2W_a, it is larger than the VBSCF value of 92.7 kcal/mol. For the S_1 state, the values of B_{σ} , B_{π} , and B_{tot} are almost unchanged compared to the gas phase results. For example, the B_{π} values of F2W_a in the S_1 state are 14.2 kcal/mol by VBEFP and 14.3 kcal/mol by VBEFP/PCM, almost the same as the value in gas phase, where the value is 14.6 kcal/mol.

Second, the π resonance dominates the variation of the total resonance in the $n \rightarrow \pi^*$ vertical excitation. For the gas phase, from the S_0 state to the S_1 state, B_{σ} is almost unchanged while B_{π} drops from 36.7 to 14.6 kcal/mol for formaldehyde and from 40.2 to 13.5 kcal/mol for acetone, which leads to the decrease of B_{tot} . The decrease of the B_{π} illustrates that the π bonding is greatly weakened due to the excitation. In the S_0 state, the B_{tot} value of acetone is somewhat larger than formaldehyde, whereas in the S_1 state, the B_{tot} value of acetone is virtually identical to formaldehyde. In aqueous solution, variations of the B_{tot} values from the S_0 state to the S_1 state are mainly attributed to the change of B_{π} value, whereas B_{σ} is almost unchanged. For example, for the F1W complex by VBEFP, the variation of the B_{tot} value from 91.8 kcal/mol in the S_0 state to 69.5 kcal/mol in the S_1 state is mainly attributed to the change of the B_{π} value from 39.3 kcal/mol in the S_0 state to 14.7 kcal/mol in the S_1 state. This change can be compared to the variation of the B_{σ} value from 42.4 kcal/mol in the S_0 state to 42.8 kcal/mol in the S_1 state.

The variation of the resonance energy in the excitation plays a key role in solvent shift, which can be understood in the following equation:

$$\text{SS}(\text{A}) = \text{SS}(\text{B}) + \Delta B_{\text{tot}} \quad (17)$$

where the solvent shift $\text{SS}(\text{A})$ can be expressed as the sum of the solvent shift from the basic VB structure ($\text{SS}(\text{B})$), and

Table 5 Resonance energies (kcal/mol) for the S_0 and the S_1 states of the $n \rightarrow \pi^*$ vertical excitation

		VBSCF	VBPCM	VBEFP				VBEFP/PCM			
		F0	F0	F1W	F2W _a	F2W _b	F2W _c	F1W	F2W _a	F2W _b	F2W _c
S_0	B_{total}	88.8	91.4	91.8	94.9	93.6	98.1	93.5	95.4	94.9	99.4
	B_π	36.7	39.3	38.2	39.8	39.2	43.8	40.0	40.6	40.5	45.1
	B_σ	41.8	42.4	43.5	45.2	44.6	44.5	43.8	45.1	44.7	44.7
S_1	B_{total}	68.4	69.0	69.5	70.9	70.3	68.9	69.9	70.9	70.5	69.2
	B_π	14.6	14.7	14.3	14.2	14.1	13.7	14.4	14.3	14.2	13.8
	B_σ	42.1	42.8	43.8	45.4	44.8	44.9	44.2	45.4	45.0	45.1
		A0	A0	A1W	A2W _a	A2W _b		A1W	A2W _a	A2W _b	
S_0	B_{total}	92.7	95.4	96.1	99.7	97.3		97.9	100.5	98.6	
	B_π	40.2	42.7	42.2	44.2	43.1		43.9	45.0	44.4	
	B_σ	42.5	43.0	44.0	45.6	44.4		44.2	45.6	44.5	
S_1	B_{total}	67.7	68.0	68.5	69.6	68.7		68.8	69.7	68.8	
	B_π	13.5	13.6	13.2	13.0	13.1		13.3	13.0	13.2	
	B_σ	43.4	43.9	44.9	46.5	45.3		45.2	46.6	45.5	

the contribution of the resonance energies (ΔB_{tot}), defined as:

$$\Delta B_{\text{tot}} = (B_{\text{tot}}^0(\text{g}) - B_{\text{tot}}^1(\text{g})) - (B_{\text{tot}}^0(\text{a}) - B_{\text{tot}}^1(\text{a})) \quad (18)$$

where the superscripts 0 and 1 denote the S_0 and S_1 states, respectively, whereas g and a denote the gas phase and the aqueous solution, respectively.

The values of SS(A), SS(B), and ΔB_{tot} are shown in Figure 4. By VBPCM, although the SS(A) values are small, the ΔB_{tot} values are mainly attributed to the total solvent shift whereas SS(B) exhibit the red shift. The VBEFP-computed ΔB_{tot} values, which range from 626 to 3065 cm^{-1} for formaldehyde and from 873 to 1751 cm^{-1} for acetone, are mainly responses to the solvent shift. The VBEFP/PCM

results are similar to VBEFP, which shows that the solvent effects enhance SS(B) and ΔB_{tot} simultaneously. In general, for all the VB computations, ΔB_{tot} dominates the solvent shifts, which shows that reference to only the basic VB structure cannot properly describe the solvent shift. Adequate description of the solvent effect increases the ΔB_{tot} values, which leads to the proper solvent shifts. These results emphasize the importance of the solute electronic polarization, similar to the conclusion of Carloni *et al.* [21] that highlights the dominant role of the polarization of the wave functions to the solvent shift.

In addition, ΔB_{tot} can be divided into the following three contributions:

$$\Delta B_{\text{tot}} = \Delta B_{\sigma-\pi} + \Delta B_{\sigma} + \Delta B_{\pi} \quad (19)$$

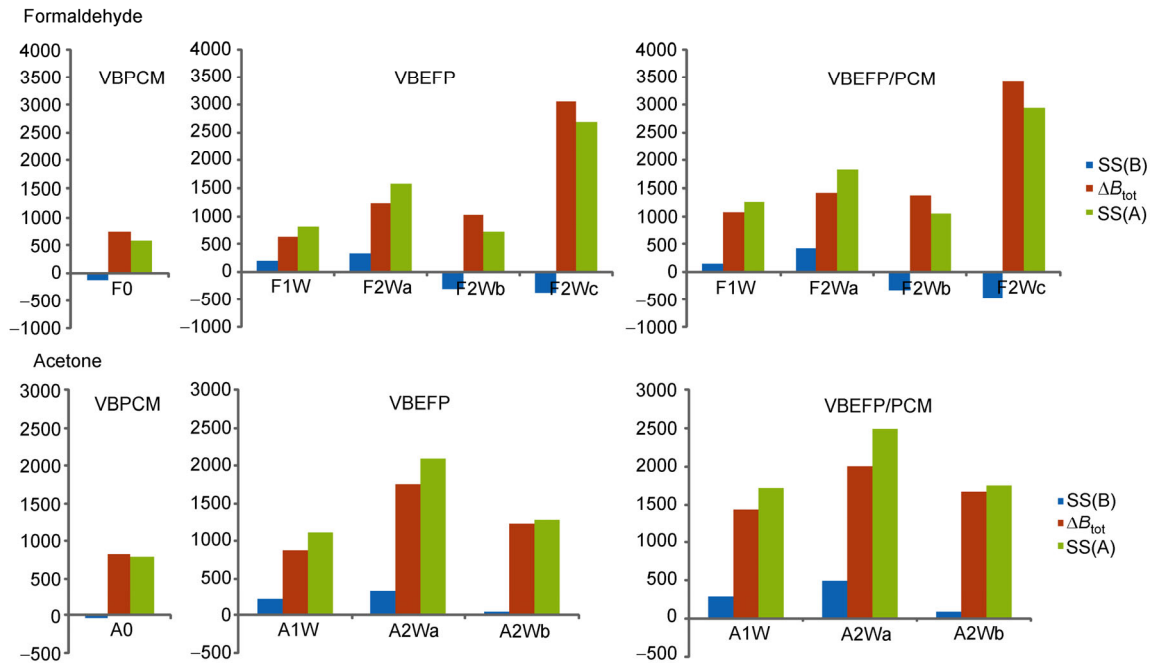
**Figure 4** Solvent shifts of CR_2O ($\text{R} = \text{H}$ or CH_3) by VBPCM, VBEFP and VBEFP/PCM.

Table 6 The ΔB_{tot} , B_{σ} , B_{π} and $B_{\sigma-\pi}$ values (cm^{-1}) by VBPCM, VBEFP, and VBEFP/PCM

	VBPCM		VBEFP			VBEFP/PCM			
	F0	F1W	F2W _a	F2W _b	F2W _c	F1W	F2W _a	F2W _b	F2W _c
ΔB_{total}	721	626	1241	1031	3065	1096	1418	1383	3417
ΔB_{π}	843	608	1197	1010	2792	1178	1464	1442	3205
ΔB_{σ}	-11	17	33	31	-18	-6	-4	10	-28
$\Delta B_{\sigma-\pi}$	-111	1	11	-10	291	-76	-42	-69	240
	A0	A1W	A2W _a	A2W _b		A1W	A2W _a	A2W _b	
ΔB_{total}	816	873	1751	1227		1433	1998	1670	
ΔB_{π}	860	803	1586	1138		1393	1863	1598	
ΔB_{σ}	-5	9	15	0		-4	-10	-7	
$\Delta B_{\sigma-\pi}$	-39	61	150	89		44	145	79	

where ΔB_{σ} , ΔB_{π} , and $\Delta B_{\sigma-\pi}$ denote the respective contributions of B_{σ} , B_{π} , and $B_{\sigma-\pi}$ to the solvent shift.

The ΔB_{tot} , B_{σ} , B_{π} , and $B_{\sigma-\pi}$ values are shown in Table 6. By VBPCM, the effect of σ resonance gives a red shift (-11 cm^{-1} for formaldehyde and -5 cm^{-1} for acetone). The ΔB_{π} values, 843 cm^{-1} for formaldehyde and 860 cm^{-1} for acetone, cover the large portion of ΔB_{tot} . By VBEFP, the ΔB_{π} values, which range from 608 to 2792 cm^{-1} for formaldehyde and from 803 to 1586 cm^{-1} for acetone, are mainly attributed to the variation of the total resonance. By VBEFP/PCM, ΔB_{π} values (from 1178 to 3205 cm^{-1} for formaldehyde and from 1393 to 1598 cm^{-1} for acetone) also response to the ΔB_{tot} values. In general, the $\Delta B_{\sigma-\pi}$ values are larger than the ΔB_{σ} , that covers the small portion of the ΔB_{tot} value. In conclusion, ΔB_{π} is the largest contributor to ΔB_{tot} . With quantificational analysis, the dominant role of the π resonance energy in the solvent shift is clarified.

5 Conclusions

In this paper, a new QM/MM/PCM type scheme, called VBEFP/PCM, is introduced for *ab initio* VB study with complicated solvent effect. In VBEFP/PCM, the QM part is handled by *ab initio* VB theory. The short-range solvent effect is considered by the EFP method, whereas the long-range solvent effect is taken into account by the PCM method. VBEFP/PCM, along with VBPCM and VBEFP, is employed for the $n \rightarrow \pi^*$ vertical excitations of formaldehyde and acetone in aqueous solution. It is validated that VBEFP/PCM can provide the appropriate solvent shifts; by contrast, VBPCM underestimates the solvent shifts due to its lack of short-range solvent effect. The VBEFP results strongly rely upon the description of the short-range solvent effect. To explore the role of the solute's electronic structure in the solvent shifts, the behavior of the resonance energy during the excitation is discussed. It is shown that the polarization of the solute's electronic structure is the most important for the solvent shift. The adequate description of the solvent effect enhances the resonance effect. Moreover, the π resonance controls the variation of the wave function

from the S_0 state to the S_1 state, which leads to the blue solvent shifts.

This project is supported by the Ministry of Science and Technology of China (2011CB808504), the Natural Science Foundation of China (21003101, 21120102035, 21273176, 21290193), and the Natural Science Foundation of Fujian Province, China (2013J01058).

- 1 Canuto S. *Solvation Effects on Molecules and Biomolecules: Computational Methods and Applications*. New York: Springer, 2008
- 2 Tomasi J, Mennucci B, Cammi R. Quantum mechanical continuum solvation models. *Chem Rev*, 2005, 105: 2999–3094
- 3 Song L, Wu W, Zhang Q, Shaik S. VBPCM: a valence bond method that incorporates a polarizable continuum model. *J Phys Chem A*, 2004, 108: 6017–6024
- 4 Su P, Wu W, Kelly CP, Cramer CJ, Truhlar DG. VBSM: a solvation model based on valence bond theory. *J Phys Chem A*, 2008, 112: 12761–12768
- 5 Tomasi J, Mennucci B, Cammi R. Quantum mechanical continuum solvation models. *Chem Rev*, 2005, 105: 2999–3094
- 6 Kelly CP, Cramer CJ, Truhlar DG. SM6: a density functional theory continuum solvation model for calculating aqueous solvation free energies of neutrals, ions, and solute-water clusters. *J Chem Theory Comput*, 2005, 1: 1133–1152
- 7 Marenich AV, Olson RM, Kelly CP, Cramer CJ, Truhlar DG. Self-consistent reaction field model for aqueous and nonaqueous solutions based on accurate polarized partial charges. *J Chem Theory Comput*, 2007, 3: 2011–2033
- 8 Warshel A. *Computer Modeling of Chemical Reactions in Enzymes and Solutions*. New York: Wiley-Interscience, 1991
- 9 Ying F, Chang X, Su P, Wu W. VBEFP: a valence bond approach that incorporates effective fragment potential method. *J Phys Chem A*, 2012, 116: 1846–1853
- 10 Gordon MS, Freitag MA, Bandyopadhyay P, Jensen JH, Kairys V, Stevens WJ. The effective fragment potential method: a QM-based MM approach to modeling environmental effects in chemistry. *J Phys Chem A*, 2000, 105: 293–307
- 11 Improta R, Barone V. Interplay of electronic, environmental, and vibrational effects in determining the hyperfine coupling constants of organic free radicals. *Chem Rev*, 2004, 104: 1231–1254
- 12 Bandyopadhyay P, Gordon MS, Mennucci B, Tomasi J. An integrated effective fragment-polarizable continuum approach to solvation: theory and application to glycine. *J Chem Phys*, 2002, 116: 5023–5032
- 13 Li H, Pomelli CS, Jensen JH. Continuum solvation of large molecules described by QM/MM: a semi-iterative implementation of the PCM/EFP interface. *Theor Chem Acc*, 2003, 109: 71–84
- 14 Blair JT, Krogh-Jespersen K, Levy RM. Solvent effects on optical absorption spectra: the $^1A_1 \rightarrow ^1A_2$ transition of formaldehyde in water. *J Am Chem Soc*, 1989, 111: 6948–6956

- 15 Lin, Gao J. Solvatochromic shifts of the $n \rightarrow \pi^*$ transition of acetone from steam vapor to ambient aqueous solution: a combined configuration interaction QM/MM simulation study incorporating solvent polarization. *J Chem Theory Comput*, 2007, 3: 1484–1493
- 16 Li H. Quantum mechanical/molecular mechanical/continuum style solvation model: linear response theory, variational treatment, and nuclear gradients. *J Chem Phys*, 2009, 131: 184103
- 17 Li YK, Zhu Q, Li XY, Fu KX, Wang XJ, Cheng XM. Spectral shift of the $n \rightarrow \pi^*$ transition for acetone and formic acid with an explicit solvent model. *J Phys Chem A*, 2010, 115: 232–243
- 18 Marenich AV, Cramer CJ, Truhlar DG. Sorting out the relative contributions of electrostatic polarization, dispersion, and hydrogen bonding to solvatochromic shifts on vertical electronic excitation energies. *J Chem Theory Comput*, 2010, 6: 2829–2844
- 19 Angeli C, Borini S, Ferrighi L, Cimiraglia R. *Ab initio* n -electron valence state perturbation theory study of the adiabatic transitions in carbonyl molecules: formaldehyde, acetaldehyde, and acetone. *J Chem Phys*, 2005, 122: 114304–114310
- 20 Improta R, Scalmani G, Frisch MJ, Barone V. Toward effective and reliable fluorescence energies in solution by a new state specific polarizable continuum model time dependent density functional theory approach. *J Chem Phys*, 2007, 127: 074504–074509
- 21 Lupieri P, Ippoliti E, Altoè P, Garavelli M, Mwalaba M, Carloni P. Spectroscopic properties of formaldehyde in aqueous solution: insights from car-parrinello and TDDFT/CASPT2 calculations. *J Chem Theory Comput*, 2010, 6: 3403–3409
- 22 Xu Z, Matsika S. Combined multireference configuration interaction/molecular dynamics approach for calculating solvatochromic shifts: application to the $n \rightarrow \pi^*$ electronic transition of formaldehyde. *J Phys Chem A*, 2006, 110: 12035–12043
- 23 Kongsted J, Osted A, Pedersen TB, Mikkelsen KV, Christiansen O. The $n \rightarrow \pi^*$ electronic transition in microsolvated formaldehyde. A coupled cluster and combined coupled cluster/molecular mechanics study. *J Phys Chem A*, 2004, 108: 8624–8632
- 24 Li J, Cramer CJ, Truhlar DG. Two-response-time model based on CM2/INDO/S2 electrostatic potentials for the dielectric polarization component of solvatochromic shifts on vertical excitation energies. *Int J Quantum Chem*, 2000, 77: 264–280
- 25 Wu W, Su P, Shaik S, Hiberty PC. Classical valence bond approach by modern methods. *Chem Rev*, 2011, 111: 7557–7593
- 26 Schmidt MW, Baldridge KK, Boatz JA, Elbert ST, Gordon MS, Jensen JH, Koseki S, Matsunaga N, Nguyen KA, Su S, Windus TL, Dupuis M, Montgomery JA. General atomic and molecular electronic structure system. *J Comput Chem*, 1993, 14: 1347–1363
- 27 Cossi M, Rega N, Scalmani G, Barone V. Energies, structures, and electronic properties of molecules in solution with the C-PCM solvation model. *J Comput Chem*, 2003, 24: 669–681
- 28 Su P, Li H. Continuous and smooth potential energy surface for conductorlike screening solvation model using fixed points with variable areas. *J Chem Phys*, 2009, 130: 074109–074109
- 29 Rappe AK, Casewit CJ, Colwell KS, Goddard WA, Skiff WM. UFF, a full periodic table force field for molecular mechanics and molecular dynamics simulations. *J Am Chem Soc*, 1992, 114: 10024–10035
- 30 Chen Z, Zhang Q, Wu W. A new algorithm for inactive orbital optimization in valence bond theory. *Sci China Ser B-Chem*, 2009, 52: 1879–1884
- 31 Chen Z, Chen X, Wu W. Nonorthogonal orbital based n -body reduced density matrices and their applications to valence bond theory. II. An efficient algorithm for matrix elements and analytical energy gradients in vbscf method. *J Chem Phys*, 2013, 138: 164120
- 32 Chen Z, Chen X, Wu W. Nonorthogonal orbital based n -body reduced density matrices and their applications to valence bond theory. I. Hamiltonian matrix elements between internally contracted excited valence bond wave functions. *J Chem Phys*, 2013, 138: 164119
- 33 Song L, Chen Z, Ying F, Song J, Chen X, Su P, Mo Y, Zhang Q, Wu W. XMVB 2.0: an *ab initio* non-orthogonal valence bond program. Xiamen: Xiamen University, 2012
- 34 Song L, Mo Y, Zhang Q, Wu W. XMVB: a program for *ab initio* nonorthogonal valence bond computations. *J Comput Chem*, 2005, 26: 514–521
- 35 Weyl H. *The Theory of Groups and Quantum Mechanics*. New York: Dover, 1950
- 36 Su P, Song L, Wu W, Hiberty PC, Shaik S. A valence bond study of the dioxygen molecule. *J Comput Chem*, 2007, 28: 185–197
- 37 Su P, Wu W, Shaik S, Hiberty PC. A valence bond study of the low-lying states of the N_2 molecule. *ChemPhysChem*, 2008, 9: 1442–1452
- 38 Su P, Wu J, Gu J, Wu W, Shaik S, Hiberty PC. Bonding conundrums in the C_2 molecule: a valence bond study. *J Chem Theory Comput*, 2010, 7: 121–130
- 39 Brand JCD. 184. The electronic spectrum of formaldehyde. *J Chem Soc (Resumed)*, 1956: 858–872
- 40 Walzl KN, Koerting CF, Kuppermann A. Electron-impact spectroscopy of acetaldehyde. *J Chem Phys*, 1987, 87: 3796–3803
- 41 Bayliss NS, McRae EG. Solvent effects in the spectra of acetone, crotonaldehyde, nitromethane and nitrobenzene. *J Phys Chem*, 1954, 58: 1006–1011
- 42 Paul S. Invited review solvatochromic shifts: the influence of the medium on the energy of electronic states. *J Photochem Photobiol A*, 1990, 50: 293–330
- 43 Bercovici T, King J, Becker RS. Formaldehyde: comprehensive spectral investigation as a function of solvent and temperature. *J Chem Phys*, 1972, 56: 3956–3963
- 44 Naka K, Morita A, Kato S. Effect of solvent fluctuation on the electronic transitions of formaldehyde in aqueous solution. *J Chem Phys*, 1999, 110: 3484–3492
- 45 Kongsted J, Osted A, Mikkelsen KV, Astrand PO, Christiansen O. Solvent effects on the $n \rightarrow \pi^*$ electronic transition in formaldehyde: a combined coupled cluster/molecular dynamics study. *J Chem Phys*, 2004, 121: 8435–8445
- 46 Bayliss NS, Wills-Johnson G. Solvent effects on the intensities of the weak ultraviolet spectra of ketones and nitroparaffins—I. *Spectrochim Acta A*, 1968, 24: 551–561
- 47 Hayes WP, Timmons CJ. Solvent and substituent effects on the $n \rightarrow \pi^*$ absorption bands of some ketones. *Spectrochimica Acta*, 1965, 21: 529–541
- 48 Crescenzi O, Pavone M, De Angelis F, Barone V. Solvent effects on the UV ($n \rightarrow \pi^*$) and NMR(^{13}C and ^{17}O) spectra of acetone in aqueous solution. An integrated car-parrinello and DFT/PCM approach. *J Phys Chem B*, 2004, 109: 445–453
- 49 Bernasconi L, Sprik M, Hutter J. Time dependent density functional theory study of charge-transfer and intramolecular electronic excitations in acetone-water systems. *J Chem Phys*, 2003, 119: 12417–12431
- 50 Gao J. Monte carlo quantum mechanical-configuration interaction and molecular mechanics simulation of solvent effects on the $n \rightarrow \pi^*$ blue shift of acetone. *J Am Chem Soc*, 1994, 116: 9324–9328